



Published in final edited form as:

Nat Commun. 2013 ; 4: 1382. doi:10.1038/ncomms2381.

Analysis of protein coding mutations in hiPSCs and their possible role during somatic cell reprogramming

Sergio Ruiz^{1,*}, Athurva Gore^{2,*}, Zhe Li², Athanasia D. Panopoulos¹, Nuria Montserrat³, Ho-Lim Fung², Alessandra Giorgetti³, Josipa Bilic³, Erika M. Batchelder¹, Holm Zaehres⁴, Hans R. Schöler⁴, Kun Zhang^{2,#}, and Juan Carlos Izpisua Belmonte^{1,3,#}

¹Gene Expression Laboratory, Salk Institute for Biological Studies, 10010 North Torrey Pines Road, La Jolla, CA 92037

²Department of Bioengineering, University of California at San Diego, 9500 Gilman Drive, La Jolla, CA, 92093, USA

³Center of Regenerative Medicine in Barcelona, Doctor Aiguader, 88, 08003 Barcelona, Spain

⁴Department of Cell and Developmental Biology, Max Planck Institute for Molecular Biomedicine, Röntgenstrasse 20, 48149 Münster, Germany

Abstract

Recent studies indicate that human induced pluripotent stem cells (hiPSCs) contain genomic structural variations and point mutations in coding regions. However, these studies have focused on fibroblast-derived hiPSCs, and it is currently unknown whether the use of alternative somatic cell sources with varying reprogramming efficiencies would result in different levels of genetic alterations. Here we characterize the genomic integrity of eight hiPSC lines derived from five different non-fibroblast somatic cell types. We show that protein-coding mutations are a general feature of the hiPSC state and are independent of somatic cell source. Furthermore, we analyze a total of 17 point mutations found in hiPSCs and demonstrate that they do not generally facilitate the acquisition of pluripotency and thus are not likely to provide a selective advantage for reprogramming.

INTRODUCTION

The induction of pluripotency in human somatic cells by defined transcription factors represents a breakthrough in regenerative medicine¹⁻⁵. The generation of patient-specific human induced pluripotent stem cells (hiPSCs) and their autologous cell derivatives would

Users may view, print, copy, download and text and data- mine the content in such documents, for the purposes of academic research, subject always to the full Conditions of use: http://www.nature.com/authors/editorial_policies/license.html#terms

#Correspondence should be addressed to: Kun Zhang (kzhang@bioeng.ucsd.edu, Tel: 858-822-7876; Fax: 858-534-5722) and Juan Carlos Izpisua Belmonte (belmonte@salk.edu/ izpisua@cibr.eu, Tel: 858-453-4100 ext: 1130).

*These authors contributed equally to this work.

AUTHOR CONTRIBUTIONS

SR, AG, KZ and JCIB designed the experiments. SR, AG, NM, AGi, JB, ADP, ZL, HF and EMB carried out experiments. HZ and HS helped with procedures. SR, AG, ADP, KZ and JCIB wrote the manuscript. KZ and JCIB directed the project and revised the manuscript. All authors provided detailed comments.

help to overcome the problems of immune rejection and tissue availability. However, the applications of cell therapies in human patients are subject to very stringent safety requirements, and there is a general concern in the field about the safety of hiPSCs.

Successful generation of hiPSCs depends on the complete reprogramming of the somatic epigenome to a pluripotent state while the genome remains unchanged. Although initial reports demonstrated that human embryonic stem cells (hESCs) and hiPSCs were very similar, recent reports have uncovered striking genetic and epigenetic differences between these two pluripotent cell types⁶⁻¹¹. It has been shown that hiPSCs display protein-coding mutations, large-scale genomic rearrangements, persistent epigenetic marks from the somatic cell type of origin and aberrant methylation patterns^{6, 9, 11}. These findings indicated that hiPSCs contain genomic defects that could preclude their use in stem cell therapies. However, most of these studies focused on fibroblast-derived hiPSCs and a more comprehensive analysis is essential to determine whether there are specific somatic cell types that may reprogram into hiPSCs with fewer (or perhaps none) of these aberrations. Additionally, it is unclear whether the protein-coding mutations found in hiPSCs provide any functional advantage and thus, are selected for during the process of reprogramming.

In this work, we characterize at single nucleotide resolution the genomic integrity of eight hiPSC lines derived from five different non-fibroblast somatic cell types with varied reprogramming efficiencies. Moreover, we functionally characterize the role of 17 point mutations found in hiPSCs for their ability to increase reprogramming efficiency. We demonstrate that the majority of these mutations do not favor the reprogramming process and suggest that most of them originated randomly or were initially present in the somatic population of origin. Our observations of the genetic abnormalities of hiPSCs will contribute to a deeper understanding of the reprogramming process.

RESULTS

hiPSC lines from varied cell types contain protein-coding mutations

We previously sequenced the protein-coding regions of 22 fibroblast-derived hiPSC lines and discovered that the hiPSCs analyzed carried between 2 and 14 point mutations in protein-coding regions⁶. In this study, we sought to determine if low reprogramming efficiency (and therefore a potentially higher level of selection pressure which could allow the fixation of advantageous mutations) or cell type of origin (as fibroblasts could possess a higher somatic mutation rate than other cell types) could contribute to the overall reprogramming-associated mutational load. To this end, we performed targeted exome sequencing on eight non-fibroblast derived hiPSC lines and their five somatic cell types of origin using an in-solution hybridization capture method (Supplementary Table S1). Somatic mutations in each hiPSC line were identified via pairwise comparison with the matched somatic cell of origin and independently confirmed with capillary Sanger sequencing. We identified a total of 40 point mutations throughout all the hiPSC lines analyzed, leading to an average of 5 coding mutations per line (Table 1). As we identified ~89% of expected total single nucleotide polymorphisms at high sequencing depth in protein-coding regions, this led to a projection of 45 total mutations in protein-coding regions, or approximately 6 coding mutations per cell line. The levels of mutational load from each individual somatic

cell type were statistically indistinguishable, and within the range previously observed for fibroblast-derived hiPSC lines⁶ (Table 1). These results indicate that hiPSC-associated mutations cannot be avoided by using younger or potentially more genetically protected somatic cell sources as progenitor cells. Moreover, we determined that reprogramming efficiency, which varies between 0.001–3% for these cell types, did not seem to have a measurable effect on the hiPSC mutational load. Thus, reprogramming-associated point mutations appear to be a general feature of hiPSCs.

We next investigated whether mutations in hiPSCs were either enriched or depleted in protein coding-regions. To this end, we examined additional non-coding regions captured in our sequencing analysis, and found a similar mutation rate per base pair analyzed for both coding and non-coding regions (Table 2). We also investigated whether point mutations in hiPSCs tended to occur in active/ubiquitous or silent/tissue-specific genes. Among a total of 132 mutated genes (from this study and Gore et al) annotated in the TiGER Database (TIssue-specific Gene Expression and Regulation)¹², 37% of these genes showed tissue-specific expression, which is very similar to the overall level of tissue specificity observed in the genes annotated in the database (34%; $p=0.4975$), indicating that mutations are not preferentially occurring in silent genes. We additionally checked for any potential enrichment of mutations in active or inactive transcriptional regions of the genome¹³. We found that mutations were not significantly enriched in the active or inactive chromatin regions of fibroblasts (p -value=0.79), hESCs (p -value=0.29), or hiPSCs (p -value=0.07). Furthermore, only one gene (*NTRK3*) was found mutated in more than one independent hiPSC line and mutated genes did not cluster in a specific functional pathway (Gore et al⁶ and results herein). These combined findings suggest that mutations in hiPSCs are spread throughout both transcriptionally active and silent regions of the genome.

hiPSC-point mutations do not favor the process of reprogramming

We previously showed that at least half of reprogramming-associated point mutations pre-exist in starting somatic cell populations at low frequency⁶. This leads to a hypothesis that a sub-population of somatic cells carrying certain mutations could be primed for reprogramming, which would be consistent with the elite model for reprogramming¹⁴. To investigate the functional potential of these mutations during reprogramming we first assessed whether mutated alleles were expressed in the hiPSC lines. We isolated RNA from 3 hiPSC lines, reverse-transcribed it into cDNA, and sequenced a total of 6 transcripts of randomly selected genes found mutated in these hiPSC lines. We detected heterozygous expression of both mutant and wild-type alleles in all cases (Fig. 1) indicating that mutated transcripts are expressed in hiPSCs.

We next sought to determine if reprogramming-associated mutations could contribute functionally in facilitating the acquisition of pluripotency during reprogramming. From a total of 164 different genes found mutated in hiPSC lines (Gore et al⁶ and this study), we assayed the function of 17 candidate genes and their mutated forms during reprogramming (Supplementary Table S2). These candidate genes were selected based on the likelihood of the mutation to change protein function, the mutation type (only nonsynonymous mutations were analyzed) and whether the gene was known to be related to the maintenance and/or

protein (wt/mut) in equal amounts with that of cells over-expressing wild-type protein alone (wt/wt). Interestingly, we did not observe any difference in reprogramming efficiency between cells over-expressing the wt/wt and wt/mut proteins (Fig. 3a). Finally, we investigated whether silencing of retroviral transgenes during reprogramming could mask a gain-of-function effect of the mutated genes at a later stage of reprogramming. To this, we analyzed the reprogramming efficiency of cells infected with retroviruses expressing OSKC, the wild type or mutated forms of the genes evaluated in this study, and a red fluorescent protein (RFP) reporter gene to monitor transgene silencing. Reprogramming efficiency was evaluated based on the number of Tra-1-60⁺/RFP⁺ colonies present at day 14. These colonies represent putative bona-fide hiPSC colonies, as they express the stem cell marker Tra-1-60 but lack silencing of the exogenous transgenes. Thus, we only considered reprogramming events where transgene expression was still active. Importantly, we did not observe differences in reprogramming efficiency between cells over-expressing the mutated forms and cells over-expressing their respective wild-type forms (Fig. 3b). Furthermore, we also evaluated reprogramming efficiency in the same experiment at day 14 by analyzing the number of Tra-1-60⁺/RFP⁻ colonies (evaluating putative bona-fide hiPSC colonies where transgene silencing occurred), and obtained a similar result (data not shown). Overall, these data suggest that most of these mutated genes do not facilitate reprogramming through a gain-of-function or loss-of-function mechanism.

DISCUSSION

Our work demonstrates that hiPSCs contain protein-coding mutations independent of the cell type of origin (as we analyzed hiPSC lines derived from five tissue types). Moreover, we determined that reprogramming efficiency, and therefore the level of selection pressure which could allow the fixation of advantageous mutations, did not have a measurable effect on the hiPSC mutational load. Although the functional consequences of individual protein-coding mutations detected in hiPSCs remain to be characterized, these alterations could potentially contribute to the functional differences observed between hiPSC lines¹⁵⁻¹⁷. Two independent groups have recently reported the whole genome sequencing of human and murine iPSC lines and their corresponding somatic cell lines¹⁸⁻¹⁹. They identified hundreds of single nucleotide variants (SNVs) in non-coding regions as well as an average of 6-12 SNVs in coding regions¹⁸⁻¹⁹, which is consistent with our results⁶. Importantly, their data suggest that much of the genetic variation in iPSC clones pre-exists in the somatic population of origin and is fixed as a consequence of cloning individual cells during iPSC generation¹⁸⁻¹⁹. Although these reports supported previous observations⁶, they did not investigate whether identified mutations contribute functionally to facilitate the acquisition of pluripotency during reprogramming.

In this work, we show evidence suggesting that most reprogramming-associated point mutations do not provide a detectable selective advantage towards a reprogrammed state. Since inhibiting wild type POLR1C expression had a positive impact on reprogramming efficiency, we cannot rule out a potential role of the mutation found in POLR1C in facilitating reprogramming. If this is the case, the fact that down-regulation of POLR1C increases reprogramming efficiency in fibroblasts but not in HUVEC could indicate the existence of tissue-specific mutations affecting reprogramming efficiency, as POLR1C^{P278R}

was found in one hiPSC line derived from human fibroblasts. Although it remains possible that untested mutated genes or a combination of mutations in a certain cellular context could play a role, the findings that only one gene (NTRK3) was found mutated in 2 out of 30 independent hiPSC lines, that mutated genes do not cluster in a specific functional pathway that could explain their selection during the reprogramming process, and that non-coding regions showed a similar mutational load, indicate that reprogramming-associated mutations seem to occur through a random process without selection and/or be initially present in the somatic population of origin^{18–19}. It has been suggested that genomic alterations (i.e. duplications, deletions and mutations) are selected for during reprogramming, yet this has not been demonstrated^{6–11}. In contrast to well-established recurrent genomic aberrations (e.g. chromosome 12 duplications) present in hESC or hiPSC lines that are functionally selected upon prolonged culture⁸, our results suggest that reprogramming-associated point mutations generally do not affect reprogramming efficiency although there could be exceptions. To our knowledge, the data provided herein provides for the first time a functional analysis of the role of specific genomic alterations (i.e. point mutations in coding regions) on the reprogramming process and have potential implications for the future of the hiPSC field in regenerative medicine.

METHODS

Cell culture

The hiPSC lines AStHiPS4F4, AStHiPS4F5, HUVhiPS4F1, HUVhiPS4F3, FhiPS4F7, NSChiPS2F and FhiPS3F1 were already described^{6, 20–22}, and obtained from existing cultures. The hiPSC lines MSChiPS4F4, MSChiPS4F8 and KhiPS4F8 show all the requirements (morphology, pluripotent gene expression, normal karyotype and *in vivo* differentiation by teratoma formation) to define them as hiPSC cell lines. Derived hiPSCs were cultured as described²⁴. 293T cells and BJ human fibroblasts (ATCC, CRL-2522) were cultured in DMEM (Invitrogen) supplemented with 10% FBS and 0.1 mM non-essential aminoacids. HUVEC cells were obtained from Lonza (C-2519A) and grown with EGM-2 media (Lonza) as recommended. MSCs were kindly provided by Cécile Volle (Sanofi-Aventis) and grown in α -MEM (Invitrogen) containing 10% FBS (Hyclone), penicillin/streptomycin, sodium pyruvate, nonessential amino acids, and L-glutamine (all from Invitrogen). Human keratinocytes were obtained and cultured as previously described²³.

hiPSC generation

To generate hiPSCs (KhiPS4F8, MSChiPS4F4 and MSChiPS4) or to evaluate reprogramming efficiency, experiments were performed as described with minor modifications²⁴. Briefly, BJ fibroblasts, keratinocytes, MSCs or HUVEC cells were infected with an equal ratio of retroviruses or retroviruses plus lentiviruses by spinfection of the cells at 1850 rpm for 1 hour at room temperature in the presence of polybrene (4 μ g/ml). After one (in case of the HUVEC cells), two (in case of the BJs fibroblasts or keratinocytes) or three (in case of the MSCs) viral infections viral infections, cells were trypsinized and transferred onto fresh irradiated mouse embryonic or human fibroblasts (iMEFs or iHFs) where correspond. One day after, cells were switched to hES cell medium (DMEM/F12 or KO-DMEM (Invitrogen) supplemented with 20% Knockout Serum Replacement

(Invitrogen), 1 mM L-glutamine, 0.1 mM non-essential amino acids, 55 μ M β -mercaptoethanol and 10 ng/ml bFGF (Joint Protein Central)). Depending on the cell type of origin, colonies were stained for Nanog expression at day 18 (in the case of HUVEC-derived hiPS cells) or 24 (in the case of BJ fibroblasts-derived hiPS cells) or isolated to establish cell lines. To calculate the efficiency of reprogramming, we plated the same number of infected HUVEC or BJ fibroblasts cells on iMEFs after the infection and the relative percentage of Nanog⁺ colonies to the value of the number of colonies generated with HUVEC or BJ fibroblasts cells infected with pLVTHM lentiviruses or GFP-expressing retroviruses correspondingly is shown.

Plasmid construction

The reprogramming plasmids pMX-*OCT4*, pMX-*SOX2*, pMX-*KLF4*, pMX-*cMyc* together with pLVTHM were obtained from Addgene (plasmids 17217, 17218, 17219, 17220 and 12247 respectively). For the construction of pMX-*NTRK3*, pMX-*FAIM3*, pMX-*POLRIC*, pMX-*GDF3* and pMX-*HK1* (fragment corresponding to the nucleotides 277-2753), specific coding region sequences were amplified by PCR from Human ORFeome library plasmids containing the corresponding cDNAs. cDNA fragments were digested with adequate restriction enzymes, purified and subcloned into linearized pMX plasmid. For the construction of pMX-*CCKBR*, pMX-*SAMD3*, pMX-*UBA2*, pMX-*TRAF6*, pMX-*MARCKSL1*, pMX-*CD1B*, pMX-*GSG1*, pMX-*NRP1*, pMX-*NEK11*, pMX-*CTSL1*, pMX-*ASB3* and pMX-*ZNF16*, specific pDONR223 plasmids from Human ORFeome library containing the corresponding cDNAs were used to transfer the cDNAs to the vector pMX-GW (Addgene, 18656). The transfer was achieved by using the Gateway LR Clonase enzyme mix (Invitrogen). The plasmids pMX-*p16*, pMX-*CDK4*, pMX-*CycD1*, pLVTHM-*CycE* and pLVTHM-*p53* were generated as described^{24, 25}. The plasmid pMX-RFP was kindly provided by Dr. Guanghui Liu (Gene Expression Laboratory, The SALK Institute, La Jolla, CA). For the introduction of specific point mutations in the coding sequences of the above genes (see Supplementary Table S2 for specific mutations) the QuickChange Site-Directed Mutagenesis kit was used (Stratagene; see Supplementary Table S3 for specific primers). For the generation of plasmids encoding shRNAs against the genes used in this study, specific oligos (see Supplementary Table S3 for specific primers) were annealed, phosphorylated with T4 kinase and ligated into MluI/ClaI-linearized pLVTHM plasmid. The design of 3 different pairs of shRNAs was carried out using the SFold software (<http://sfold.wadsworth.org/>) and knockdown efficiency was assayed in 293T cells. The most efficient pairs of shRNAs were assayed in HUVEC or BJ fibroblasts cell (Supplementary Fig. S1a) and used in the corresponding experiments. All constructs generated were subjected to direct sequencing to rule out the presence of mutations.

Retroviral and lentiviral production

Moloney-based retroviral vectors (pMX and derived) and second generation lentiviral vectors (pLVTHM and derived) were co-transfected with packaging plasmids to generate viral particles in 293T cells using Lipofectamine (Invitrogen) as previously described²⁴.

Immunostaining

Immunofluorescence analysis for the detection of pluripotent markers in hiPSCs or for the detection of differentiation-associated markers in teratomas were performed as described²². Immunohistochemical/immunofluorescence detection of Nanog or Tra-1-60 was performed as described²⁴.

RNA isolation and real time-PCR analysis

Total RNA was isolated using Trizol Reagent (Invitrogen) according to the manufacturer's recommendations. cDNA was synthesized using the SuperScript II Reverse Transcriptase kit for RT-PCR (Invitrogen) or the RT Supermix M-MuLV kit (BioPioneer). Real-time PCR was performed using the SYBR-Green PCR Master mix (Applied Biosystems) in the ViiA 7 Real Time PCR System (Applied Biosystems). GAPDH expression was used to normalize values of gene expression and data is shown as fold change relative to the value of the sample control. All the samples were done in triplicate. Primers used for real time-PCR experiments are listed in Supplementary Table S3.

Whole genome library construction

Library construction was performed as previously described^{6, 26}. Briefly, for each sample, roughly 1.5 to 3 µg of genomic DNA (in 100 µl volumes) was sheared with a Covaris AFA. The fragmented genomic DNA was end repaired, A-tailed, and ligated to sequencing adaptors, with a purification step between each process. The purified ligated products were then amplified by PCR to generate whole-genome libraries.

In-Solution Hybridization capture with DNA baits

Liquid exome capture was performed as previously described⁶.

Consensus sequence generation and variant calling

Variant calling was performed as previously described⁶. Briefly, reads obtained from the Illumina Genome Analyzer were post-processed and quality filtered using GERALD, mapped to the genome using BWA, downsampled using Picard, and used to generate a consensus sequence for each sample using GATK. The consensus sequences were then compared to find candidate novel mutations in hiPSCs⁶. Sites where each hiPSC line showed heterozygous SNPs not observed in the progenitor line were considered as candidate mutations if no allelic content was present in the somatic progenitor and if the candidate mutation had not previously been observed in other samples or the dbSNP database.

Sanger validation of candidate mutations

Genomic DNA of both the hiPSC line and its somatic progenitor (6 ng each) was amplified in separate 50 µl PCR reactions with 100 nM of specifically designed forward and reverse primers around the mutation site (primers available under request) and 25 µl of Taq 2x master mix (NEB) at 94 °C for 2 minutes, followed by 35 cycles of 94 °C for 30 seconds; 57 °C for 30 seconds; and 72 °C for 30 seconds, and final extension at 72 °C for 3 minutes. The PCR products were then purified with Qiagen Qiaquick columns, and 10 ng of purified

DNA was pre-mixed with 25 pmol of the forward primer for Sanger sequencing at Genewiz Inc.

Statistical Analysis/TiGER Database

To check for enrichment of reprogramming-associated mutations in genes that are expressed in a tissue-specific manner, the fraction of UniGene IDs corresponding to mutated genes called as “tissue-specific” in the TiGER database was identified as 49/132 (37%). As 6,699/19,526 (34%) of the genes annotated in the TiGER database are considered to be tissue-specific, a χ^2 test with one degree of freedom can be used to test for equivalency of distribution. The obtained χ^2 value is 0.460, indicating that the fraction of mutated hiPSC genes that are tissue-specific is not significantly different than that found in a random sample of genes (P-value = 0.4975). Reprogramming-associated mutations therefore do not appear to be enriched in tissue-specific genes.

Statistical Analysis/Active and Inactive Chromatin States

To check for enrichment of reprogramming-associated mutations in active or inactive chromatin, we utilized a χ^2 test with three degrees of freedom to test for equivalency of distribution. We identified the chromatin state of each mutated gene using previously published data¹³. This data divided each gene into one of four categories: no trimethylation, H3K4 Trimethylation, H3K27 Trimethylation, or both. We compared the distribution of mutated genes across each of these four categories with the expected distribution for all genes in three cell types: Fibroblasts, ESCs, and iPSCs¹³. The obtained χ^2 values were 1.03 (p-value=0.79), 3.78 (p-value=0.29), and 6.97 (p-value=0.07), respectively, indicating that the distribution of mutated hiPSC genes in each chromatin region is not significantly different than expected by random chance (alpha=0.01). Reprogramming-associated mutations therefore do not appear to be enriched in active or inactive chromatin states.

Non-coding versus Coding mutations

To compare the mutation rates per base pair in coding and non-coding regions of the genome, variant calling was performed as above on non-coding regions of the genome surviving library enrichment in eight hiPSC lines and their progenitor lines. The mutation rate per base pair was then estimated by dividing the number of candidate coding and non-coding mutations by the number of exomic and non-coding base pairs covered. The average coding and non-coding mutation rates were compared.

Supplementary Material

Refer to Web version on PubMed Central for supplementary material.

Acknowledgments

We express our gratitude to Travis Berggren, Margaret Lutz and Veronica Modesto for their support at the Salk Institute-Stem Cell Core, to Joaquin Sebastian for critically reading the manuscript, to Guanghui Liu for sharing reagents and to the rest of the Belmonte lab. AG was supported by the Focht-Powell Fellowship and a CIRM predoctoral fellowship. Work in this manuscript was supported by grants from Fundacion Cellex, TERCEL-ISCIIM-MINECO, Sanofi, National Institutes of Health and the G. Harold and Leila Y. Mathers Charitable Foundation.

References

1. Takahashi K, et al. Induction of pluripotent stem cells from adult human fibroblasts by defined factors. *Cell*. 2007; 131:861–872. [PubMed: 18035408]
2. Yu J, et al. Induced pluripotent stem cell lines derived from human somatic cells. *Science*. 2007; 318:1917–1920. [PubMed: 18029452]
3. Lowry WE, et al. Generation of human induced pluripotent stem cells from dermal fibroblasts. *Proc Natl Acad Sci*. 2008; 105:2883–2888. [PubMed: 18287077]
4. Meissner A, Wernig M, Jaenisch R. Direct reprogramming of genetically unmodified fibroblasts into pluripotent stem cells. *Nat Biotechnol*. 2007; 25:1177–1181. [PubMed: 17724450]
5. Park IH, et al. Reprogramming of human somatic cells to pluripotency with defined factors. *Nature*. 2008; 451:141–146. [PubMed: 18157115]
6. Gore A, et al. Somatic coding mutations in induced pluripotent stem cells. *Nature*. 2011; 471:63–67. [PubMed: 21368825]
7. Hussein SMI, et al. Copy number variation and selection during reprogramming to pluripotency. *Nature*. 2011; 471:58–62. [PubMed: 21368824]
8. Mayshar Y, et al. Identification and classification of chromosomal aberrations in human induced pluripotent stem cells. *Cell Stem Cell*. 2010; 7:521–531. [PubMed: 20887957]
9. Lister R, et al. Hotspots of aberrant epigenetic reprogramming in human induced pluripotent stem cells. *Nature*. 2011; 471:86–73.
10. Laurent LC, et al. Dynamic changes in the copy number of pluripotency and cell proliferation genes in ESCs and iPSCs during reprogramming and time in culture. *Cell Stem Cell*. 2011; 8:106–118. [PubMed: 21211785]
11. Ohi Y, et al. Incomplete DNA methylation underlies a transcriptional memory of somatic cells in human iPS cells. *Nat Cell Biol*. 2011; 13:541–549. [PubMed: 21499256]
12. Liu X, Yu X, Zack DJ, Zhu H, Qian J. TiGER: a database for tissue-specific gene expression and regulation. *BMC Bioinformatics*. 2008; 9:271. [PubMed: 18541026]
13. Guenther MG, et al. Chromatin Structure and Gene Expression Programs of Human Embryonic and Induced Pluripotent Stem Cells. *Cell Stem Cell*. 2010; 7:249–257. [PubMed: 20682450]
14. Yamanaka S. Elite and stochastic models for induced pluripotent stem cell generation. *Nature*. 2009; 460:49–52. [PubMed: 19571877]
15. Feng Q, et al. Hemangioblastic derivatives from human induced pluripotent stem cells exhibit limited expansion and early senescence. *Stem Cells*. 2010; 28:704–712. [PubMed: 20155819]
16. Hu BY, et al. Neural differentiation of human induced pluripotent stem cells follows developmental principles but with variable potency. *Proc Natl Acad Sci U S A*. 2010; 107:4335–4340. [PubMed: 20160098]
17. Miura K, et al. Variation in the safety of induced pluripotent stem cell lines. *Nat Biotechnol*. 2009; 27:743–745. [PubMed: 19590502]
18. Cheng L, et al. Low incidence of DNA sequence variation in human induced pluripotent stem cells generated by nonintegrating plasmid expression. *Cell Stem Cell*. 2012; 10:337–44. [PubMed: 22385660]
19. Young MA, et al. Background mutations in parental cells account for most of the genetic heterogeneity of induced pluripotent stem cells. *Cell Stem Cell*. 2012; 10:570–82. [PubMed: 22542160]
20. Kim JB, et al. Direct reprogramming of human neural stem cells by OCT4. *Nature*. 2009; 461:649–643. [PubMed: 19718018]
21. Panopoulos AD, et al. Rapid and highly efficient generation of induced pluripotent stem cells from human umbilical vein endothelial cells. *Plos One*. 2011; 6(5):e19743. [PubMed: 21603572]
22. Ruiz S, et al. High efficient generation of induced pluripotent stem cells from astrocytes. *Plos One*. 2010; 5(12):e15526. [PubMed: 21170306]
23. Aasen T, et al. Efficient and rapid generation of induced pluripotent stem cells from human keratinocytes. *Nat Biotechnol*. 2008; 26:1276–1284. [PubMed: 18931654]

24. Ruiz S, et al. A high proliferation rate is required for somatic cell reprogramming and maintenance of human embryonic stem cell identity. *Current Biology*. 2010; 21:45–52. [PubMed: 21167714]
25. Kawamura T, et al. Linking the p53 tumour suppressor pathway to somatic cell reprogramming. *Nature*. 2009; 460:1140–1144. [PubMed: 19668186]
26. Quail MA, Swerdlow H, Turner DJ. Improved protocols for the illumina genome analyzer sequencing system. *Curr Protoc Hum Genet*. 2009; Chapter 18(Unit 18):12.

Author Manuscript

Author Manuscript

Author Manuscript

Author Manuscript

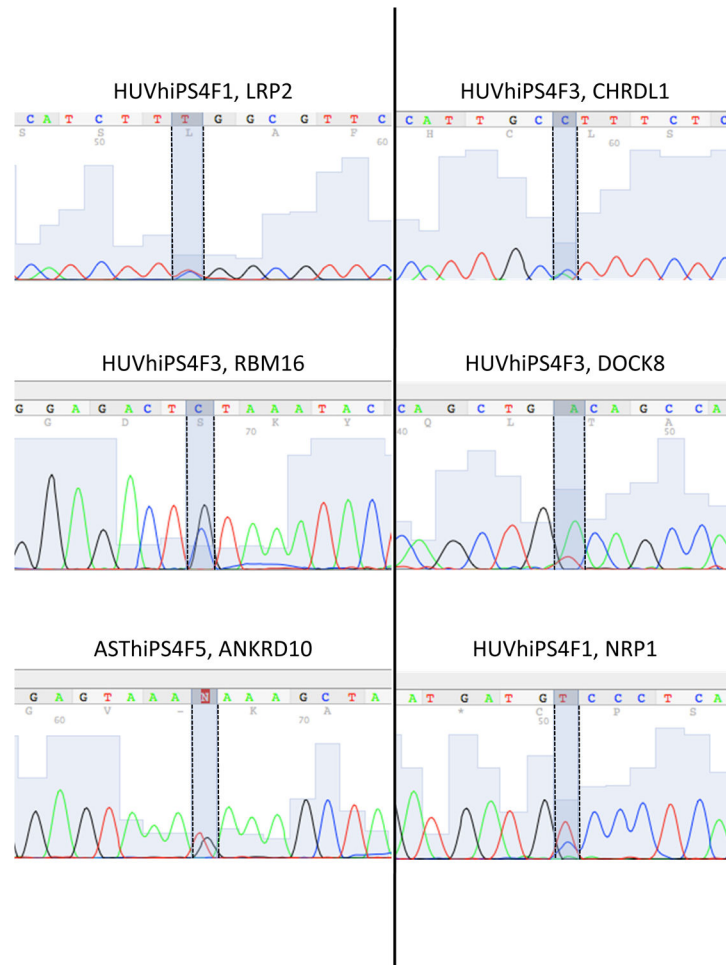
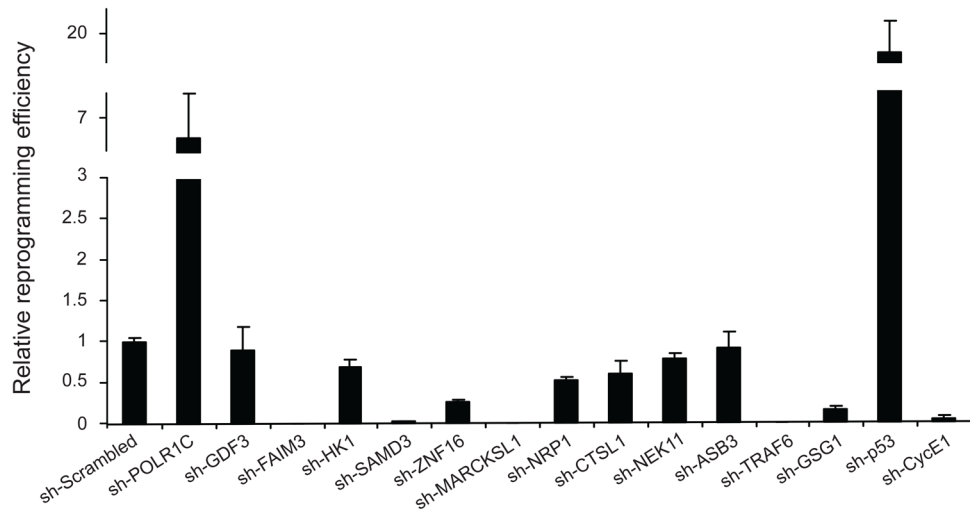


Figure 1. Mutated alleles are expressed in hiPSC lines

Sanger chromatograms showing the results of RNA Sequencing analysis performed on the indicated genes found mutated in the indicated hiPSC lines. Dashed lines highlight the point-mutated nucleotide. Note the expression of both reference and mutated alleles in all cases analyzed.

a



b

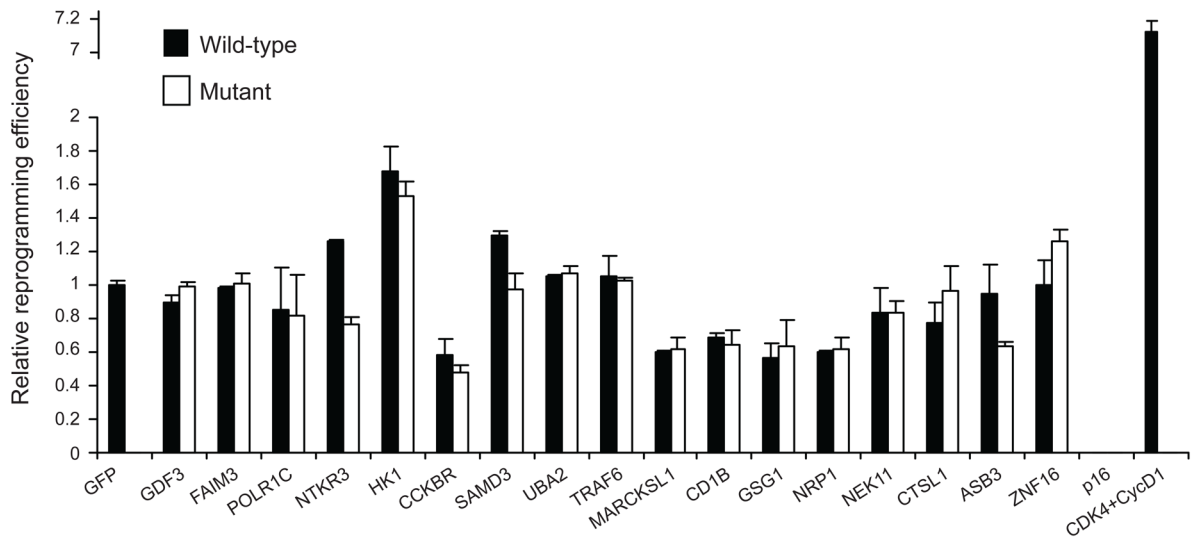


Figure 2. Evaluation of the functional effect of hiPSC mutations on reprogramming efficiency (a, b) Human BJ fibroblasts were infected with retroviruses encoding OSKC, and either lentiviruses encoding shRNAs against the indicated proteins (a) or retroviruses encoding the wild type or mutated proteins (b). Relative reprogramming efficiencies (evaluated as percentage of Nanog⁺ colonies) are shown as fold change normalized to the averaged efficiency observed in pLVTHM (a) or pMX-GFP (b) infected fibroblasts. In (a) lentiviruses encoding shRNAs against *CycE1* or *p53* were used as controls of reduced or increased reprogramming efficiency, respectively. In (b) retroviruses encoding *p16* or the pair *CDK4/CycD1* were used as controls of reduced or increased reprogramming efficiency, respectively. For (a), 20,000 infected cells were plated when shRNAs against *POLR1C* and

p53 were used and 70,000 infected cells were plated under all other conditions. For **(b)**, a total of 25,000 infected cells were plated under all conditions. Two independent experiments with two biological replicates were carried out. All error bars depict the standard deviation.

Author Manuscript

Author Manuscript

Author Manuscript

Author Manuscript

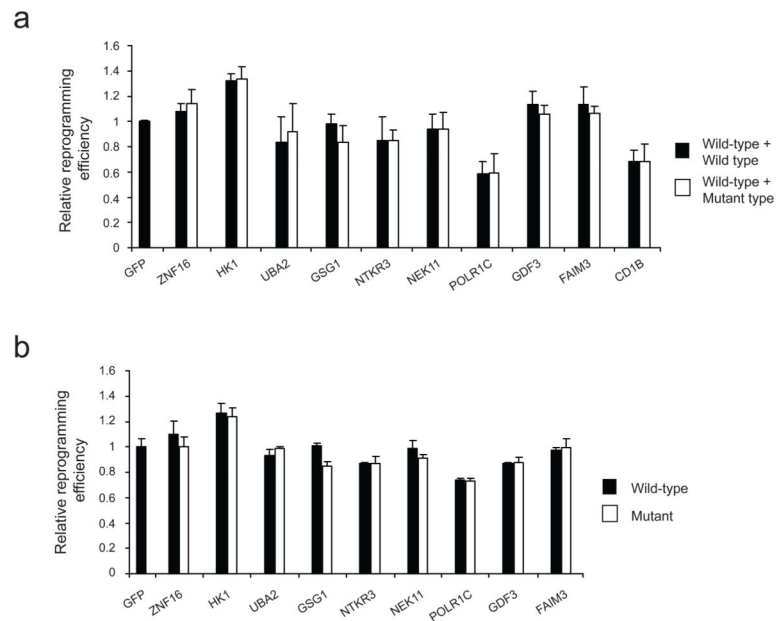


Figure 3. Retroviral silencing or wild-type/mutant gene ratio do not alter reprogramming efficiency

(a) HUVEC cells were infected with retroviruses encoding OSKC, and a similar total amount of retroviruses encoding only the wild type form or both, the wild-type (wt) and mutant (mut) forms of the protein in an equal proportion. (b) HUVEC cells were infected with retroviruses encoding OSKC, red fluorescence protein (RFP) and the wild type or mutated forms of the genes indicated. Relative reprogramming efficiencies (evaluated as percentage of Tra-1-60⁺ colonies) are shown as fold change normalized to the averaged efficiency observed in GFP-infected HUVECs. 10,000 infected cells were plated under all the conditions. Two independent experiments with two biological replicates were carried out. All error bars depict the standard deviation.

Table 1

List of protein-coding mutations in hiPSC lines

Sample	Chrom.	Position	Gene	Alleles	Protein Change	Mutation Type	SIFT Functional Prediction	Mutated in Cancer?
ASThiPS4F4	6	31783527	LY6G6F	GAC-GA	D122D	Synonymous	N/A	Yes
ASThiPS4F4	8	68087821	LRRRC67	CTT-aTT	L121I	Nonsynonymous	TOLERATED	No
ASThiPS4F5	11	54891946	OR4A15	CTG-CcG	L4P	Nonsynonymous	DAMAGING	No
ASThiPS4F5	13	110343392	ANKRD10	AAG-AAI	K225N	Nonsynonymous	TOLERATED	Yes
KhiPS4F8	1	205153901	FAIM3	TTC-aTC	F67I	Nonsynonymous	DAMAGING	Yes
KhiPS4F8	5	121215932	FTMT	CAC-CAI	H125H	Synonymous	N/A	Yes
KhiPS4F8	14	62486817	KCNH5	GAC-aAC	D386N	Nonsynonymous	TOLERATED	No
NSChiPS2F	5	79774746	ZFYVE16	TCT-TaT	S823Y	Nonsynonymous	DAMAGING	No
NSChiPS2F	12	54853783	SMARCC2	CCA-CCg	P538P	Synonymous	N/A	Yes
HUWhiPS4F1	2	169809670	LRP2	TCG-TtG	S1070L	Nonsynonymous	TOLERATED	Yes
HUWhiPS4F1	10	33542444	NRP1	GGC-GaC	G497D	Nonsynonymous	DAMAGING	No
HUWhiPS4F1	16	17139792	XYLT1	AAG-AgG	K562R	Nonsynonymous	TOLERATED	No
HUWhiPS4F1	4	155376303	DCHS2	GGA-GtA	G2529V	Nonsynonymous	DAMAGING	No
HUWhiPS4F3	6	155183150	RBM16	GTA-cTA	V595L	Nonsynonymous	TOLERATED	No
HUWhiPS4F3	9	394921	DOCK8	TCA-aCA	S1012T	Nonsynonymous	TOLERATED	Yes
HUWhiPS4F3	X	109889590	CHRD1	CTT-aTT	L86I	Nonsynonymous	TOLERATED	No
HUWhiPS4F3	19	7475243	C19orf45	TCA-TaA	S229*	Nonsense	N/A	Yes
MSChiPS4F4	1	35998698	CLSPN	GTC-ttG	V471L	Nonsynonymous	TOLERATED	Yes
MSChiPS4F4	1	153185686	PBXIP1	GAC-GgC	D363G	Nonsynonymous	TOLERATED	Yes
MSChiPS4F4	2	154960801	GALNT13	GAA-GA-g	E403E	Synonymous	N/A	Yes
MSChiPS4F4	5	126704124	MEGF10	GTC-GTg	V74V	Synonymous	N/A	Yes
MSChiPS4F4	6	130572400	SAMD3	ATG-ttG	M106L	Nonsynonymous	DAMAGING	Yes
MSChiPS4F4	10	42974297	CSGALNACT2	ATG-gtG	M264V	Nonsynonymous	TOLERATED	Yes
MSChiPS4F4	11	36473107	TRAF6	GAA-aAA	E225K	Nonsynonymous	DAMAGING	Yes
MSChiPS4F4	17	50475673	STXBP4	GTA-GTg	V236V	Synonymous	N/A	Yes
MSChiPS4F4	19	40938581	HSPB6	TCGCCG-TcAtCG	S84S P85S	Synonymous Nonsynonymous	N/A DAMAGING	No
MSChiPS4F4	20	46706999	PREX1	GCC-GCt	A703A	Synonymous	N/A	Yes
MSChiPS4F4	21	39493296	BRWD1	AAA-AIA	K1639I	Nonsynonymous	DAMAGING	Yes

Sample	Chrom.	Position	Gene	Alleles	Protein Change	Mutation Type	SIFT Functional Prediction	Mutated in Cancer?
MSChiPS4F4	X	11688927	MSL3	TCT-TTT	S111F	Nonsynonymous	DAMAGING	Yes
MSChiPS4F8	1	39703363	MACF1	GGC-IGC	G5698C	Nonsynonymous	DAMAGING	Yes
MSChiPS4F8	1	158594563	NCSTN	TTG-cTG	L670L	Synonymous	N/A	No
MSChiPS4F8	1	231873806	KCNK1	GAC-GAt	D224D	Synonymous	N/A	Yes
MSChiPS4F8	2	21087987	APOB	CAC-CgC	H1753R	Nonsynonymous	DAMAGING	Yes
MSChiPS4F8	2	234287122	UGT1A8	GTC-GaC	V249D	Nonsynonymous	N/A	Yes
MSChiPS4F8	5	128390915	SLC27A6	GAC-GAa	D482E	Nonsynonymous	DAMAGING	No
MSChiPS4F8	8	16079769	MSR1	CCG-ICG	P34S	Nonsynonymous	TOLERATED	Yes
MSChiPS4F8	9	125834763	LHX2	GAG-tAG	E393*	Nonsynonymous	N/A	No
MSChiPS4F8	14	46496570	MDGA2	TTG-aTG	L318M	Nonsynonymous	TOLERATED	Yes
MSChiPS4F8	15	37669438	THBS1	TGC-TGt	C689C	Synonymous	N/A	Yes
MSChiPS4F8	X	152498688	ATP2B3	TCC-TaC	S1134Y	Nonsynonymous	DAMAGING	Yes

Table 2

List of candidate non-coding mutations in hiPSC lines. The mutation rate per base pair was similar for exonic and non-exonic regions.

Cell Line	Noncoding Mutations			Exon Mutation Rate (per bp)	Non-exon Mutation Rate (per bp)
	Chromosome	Position	Mutation		
ASThiPS4F4	9	111225067	C -> T	8.0E-08	6.2E-08
	11	64089233	G -> T		
	13	38444609	C -> T		
ASThiPS4F5	2	114429763	A -> T	8.0E-08	1.0E-07
	12	55133583	G -> T		
	16	2290223	G -> T		
	17	40078501	C -> T		
	5	149190453	C -> A		
FIP3F1	9	5175241	C -> T	1.6E-07	1.6E-07
	10	45274877	G -> T		
	11	85134161	T -> C		
	19	48465587	C -> A		
FIP3F7	1	171784008	C -> A	1.2E-07	1.3E-07
	2	116251932	C -> A		
	2	189575154	C -> A		
	9	98839743	G -> A		
HUVhiPS4F1	11	17069813	G -> A	1.6E-07	7.2E-08
	19	21056778	G -> A		
HUVhiPS4F3	2	102515666	G -> T	1.6E-07	1.1E-07
	11	12908191	G -> T		
	15	25902050	G -> A		
	22	18130926	C -> T		
KhiPS4F8	5	96143123	C -> T	1.2E-07	1.8E-07
	9	122778753	A -> T		

Cell Line	Noncoding Mutations			Exon Mutation Rate (per bp)	Non-exon Mutation Rate (per bp)
	Chromosome	Position	Mutation		
NSChiPS2F	10	85962168	C->G	8.0E-08	1.2E-07
	17	71457091	T->C		
	5	110120401	G->T		
	9	115077723	C->T		
	9	127398270	C->T		
	11	9457743	T->A		
	19	46045755	T->G		
	1	6092988	C->G		
	2	88885962	C->T		
	2	230820856	T->C		
	3	51088015	G->T		
	4	67994660	T->A		
	4	156930655	C->A		
	5	156683693	G->C		
	6	73887041	C->T		
	6	129865735	A->G		
	8	24379410	T->A		
	10	94807938	T->C		
	10	100179495	G->A		
14	104534424	G->A			
15	61826051	G->A			
18	9551942	C->T			
X	70543403	T->C			
X	152791107	A->T			
MSChiPS4F4	1	39703363	G->T	4.8E-07	4.2E-07
	1	46422702	G->C		
	1	74608556	C->A		
	1	85589993	A->G		
	2	88885962	C->T		
MSChiPS4F8	1	39703363	G->T	4.4E-07	6.5E-07
	1	46422702	G->C		
	1	74608556	C->A		
	1	85589993	A->G		
	2	88885962	C->T		

Cell Line	Noncoding Mutations			Exon Mutation Rate (per bp)	Non-exon Mutation Rate (per bp)
	Chromosome	Position	Mutation		
	2	128062632	A -> T		
	3	12183849	G -> A		
	4	3200574	C -> T		
	4	95415046	A -> G		
	4	144675426	G -> T		
	6	37430075	G -> T		
	6	90653308	G -> T		
	6	134570140	T -> C		
	7	37123316	T -> C		
	7	117661660	A -> C		
	9	15258029	C -> G		
	9	132317600	C -> G		
	14	29171707	C -> A		
	14	73445929	C -> G		
	16	20968574	C -> T		
	16	34177914	C -> T		
	17	7778980	G -> A		
	17	62783815	G -> A		
	18	6877390	C -> T		
	19	43784039	C -> A		
	X	138470822	G -> A		
AVERAGE				1.9E-07	2.0E-07